Original Article

Genome-wide analysis of Chinese keloid patients identifies novel causative genes

Yue-Qian Zhu[1#], Nai-Hui Zhou[1#], Ya-Wen Xu[2#], Ke Liu[3], Wei Li[4], Li-Yan Shi[4], Yin-Xi Hu[4], Yu-Feng Xie[4], Jing Lan[5], Zheng-Yuan Yu[4]

[1]Department of Dermatology, The First Affiliated Hospital of Soochow University, Suzhou, China; [2]Department of Dermatology, The Third Affiliated Hospital of Soochow University, Changzhou, China; [3]Department of Dermatology, Shanghai Ninth People's Hospital, Shanghai Jiao Tong University School of Medicine, Shanghai, China; [4]Department of Oncology, The First Affiliated Hospital of Soochow University, Suzhou, China; [5]Department of General Surgery, The First Affiliated Hospital of Soochow University, Suzhou, China

Contributions: (I) Conception and design: YQ Zhu, ZY Yu; (II) Administrative support: NH Zhou, J Lan; (III) Provision of study materials or patients: YQ Zhu; (IV) Collection and assembly of data: YQ Zhu, NH Zhou, ZY Yu; (V) Data analysis and interpretation: YQ Zhu, YW Xu, ZY Yu; (VI) Manuscript writing: All authors; (VII) Final approval of manuscript: All authors.

[#]These authors contributed equally to this work.

Correspondence to: Zheng-Yuan Yu. Department of Oncology, The First Affiliated Hospital of Soochow University, Suzhou 215006, China. Email: zyyu@suda.edu.cn; Jing Lan. Department of General Surgery, the First Affiliated Hospital of Soochow University, Suzhou 215006, China. Email: drchouj@163.com.

Background: Keloids are benign skin tumors that appears on skin lesions in humans. Keloids are characterized by invasive tumor growth and are highly prone to recurrence after treatment. The incidence of keloids is ethnically specific; however, the molecular mechanism underlying the incidence of keloids in the Chinese population remains unclear. To date, no reports appear to have been published on the molecular characteristics underlying keloids in the Chinese population from the perspective of whole-genome sequencing.

Methods: In this study, we collected keloid samples from 9 keloid patients underwent surgery in the Department of Dermatology, The First Affiliated Hospital of Soochow University, paired them to normal skin tissues, and performed whole-exome sequencing. The average depth of the samples was 1,200×, and the average exome coverage was 98.90%.

Results: The bioinformatics analysis identified 3,125 single nucleotide variants (SNVs) and 299 insertions/deletions (InDels). The major mutation characteristics of the SNVs were C > A and C > T. The non-synonymous SNV types included stopgain, and stoploss. The non-synonym InDels included frameshift deletion, frameshift insertion, and stopgain. We also found a total of 67,873 copy number variations (CNVs) in the samples. The genes with the highest mutation frequency included mucin 4 (MUC4) (55.6%), tubulin tyrosine ligase like 12 (TTLL12) (33.3%), calcium voltage-gated channel subunit alpha1 (CACNA1C) (33.3%), and mucin 12 (MUC12) (33.3%). The average tumor mutation burden (TMB) was 289 mutations/million base pair (MB). The Kyoto Encyclopedia of Genes and Genomes (KEGG) pathway analysis revealed that the mutated genes were mainly concentrated in micro ribonucleic acids in cancer and the calcium signaling pathway. The Gene Ontology (GO) analysis showed that mutant genes were mainly concentrated in binding cells, cell parts, and cellular processes.

Conclusions: Whole-exome sequencing was performed in the Chinese keloid patients and some potential candidate genes related to keloid occurrence and development were identified, which may provide new molecular targets for the clinical diagnosis and treatment of keloid patients.

Keywords: Keloid; mucin 4 (MUC4); tubulin tyrosine ligase like 12 (TTLL12)

Submitted Sep 24, 2021. Accepted for publication Aug 02, 2022.
doi: 10.21037/atm-22-1303
View this article at: https://dx.doi.org/10.21037/atm-22-1303

Introduction

Keloids are hyper-fiber proliferation caused spontaneously by sensitive bodies or secondary skin trauma (e.g., from surgery, folliculitis, or varicella). Keloids grow like tumors, show invasive growth, invade normal skin, and are susceptible to drug resistance and recurrence (1). The incidence of keloids is higher in black and Hispanic people (the incidence varies from 4.5–6.2% to 16%) (2), Asians and Caucasians generally less than 1% (3,4). Keloids continue to grow, affect the appearance, may cause persistent itching, pain, and repeated infections, and seriously affect the quality of life of patients. Keloids may be caused by the mutual influence of environment, gene, or various other factors. Among them, gene variation may play a more important role in the occurrence and development of Keloids. It would be of great scientific value to accurately understand the mechanism underling keloid occurrence.

Genetic variation is an important factor in the occurrence and development of many diseases. High-throughput sequencing has been widely used in the study of a variety of complex diseases due to its advantages, such as its short consumption time, high throughput, high accuracy, and ability to screen a large number of genes at 1 time, Human whole exome sequencing is a technique to capture and enrich the DNA in the exon region of the whole human genome, and to find genetic mutations related to protein functional variation through high-throughput sequencing (5-7). Some characteristic mutated genes, such as BRAF (v-raf murine sarcoma viral oncogene homolog B1) and RAF (rat sarcoma viral oncogene homolog), have been identified in melanoma, and highly effective therapies have been developed to target these mutated genes (8,9). Li *et al.* observed the polygenic map of keloid fibroblasts of keloid fibroblasts at the level of genome differential expression (10). However, the genomic variation of keloids remains unclear. In this study, keloid tissues from 9 keloid patients underwent surgery paired with normal skin tissues at the Department of Dermatology, The First Affiliated Hospital of Soochow University and whole-exome sequencing was performed to analyze the genomic variation characteristics of the Chinese keloid patients. Related pathogenic genes, the tumor mutation burden (TMB), related molecular functions, and signaling pathways were examined. Our findings should extend understandings of keloid genesis and development, which may provide new pathway for the clinical diagnosis and treatment of keloid patients.

We present the following article in accordance with the STREGA reporting checklist (available at https://atm.amegroups.com/article/view/10.21037/atm-22-1303/rc).

Methods

Patient sample acquisition

Specimens were collected from patients undergoing keloid surgery at The First Affiliated Hospital of Soochow University from June 2019 to July 2020. The samples were taken from keloid skin near the edge of the keloid and normal skin next to the keloid. The samples were then placed in a liquid nitrogen tank. The residual keloids were taken for pathological examination, and the results conformed all the lesions were keloids. All patients were treated with radiotherapy to prevent recurrence. To be eligible for inclusion in this study, patients had to meet the following inclusion criteria: (I) have a pathological diagnosis of keloids; (II) have received no treatment in the last 6 months; (III) have consented to data collection; (IV) have signed informed consent forms. This study was conducted in accordance with the Declaration of Helsinki (as revised in 2013), and was approved by the Ethics Committee of The First Affiliated Hospital of Soochow University (application No. 2022014). Informed written consent was provided by all patients before their inclusion in this study.

DNA extraction

Deoxyribonucleic acid (DNA) was extracted using the QIAamp Fast DNA Tissue Kit (Qiagen) and QIAamp DNA FFPE Tissue kit (Qiagen). DNA extracted from normal skin tissues was used as a germline DNA control. cell populations of keloid samples were examined by pathologists, above 75% of cells were confirmed to keloid cells.

DNA quantification was performed using an Agilent's BioAnalyzer (USA).

Whole-exome sequencing

The whole-exome sequencing was conducted using the Illumina X-ten system (Illumina, San Diego, CA, USA).

Somatic SNV and InDel identification

The Burrows-Wheeler Aligner (BWA) (11) was used to

Table 1 Clinic pathological characteristics of all keloid patients

Characteristics	No. of cases
Total number	9
Age, years [mean, range]	33 [19–47]
Sex, n (%)	
Male	4 (44.0)
Female	5 (56.0)
Pathological diagnosis, n (%)	
Keloid	9 (100.0)
Keloid site of growth, n (%)	
Back	2 (22.0)
Chest	6 (67.0)
Front of the ear	1 (11.0)

align the clean reads from each sample against the human reference genome (GRCh38) and identify somatic single nucleotide variants (SNVs) and insertions/deletions (InDels). Somatic SNV and InDel calling was performed on multi-samples using MuTect (12).

Gene functional enrichment analysis

The screened gene sets were used in the functional annotation analysis using an in-house script from the Kyoto Encyclopedia of Genes and Genomes (KEGG) (13) and Gene Ontology (GO) (14) databases. A modified Fisher's exact test was used to define the significance of gene group enrichment, and a P value <0.05 was considered statistically difference.

Statistical analyses

SPSS (IBM Corp., Armonk, NY, USA) (15) was used for all the statistical analyses.

Results

Patient characteristics

The mean age of the 9 keloid patients was 33 years old (range, 19–47 years old); 4 of the patients were male and 5 were female. All patients were diagnosed with keloids. 2 patients had keloids on their backs, 6 had keloids on their chests, and 1 had a keloid on the front of their ear (see *Table 1*).

Whole-exome sequencing

Whole-exome sequencing was performed on the normal tissue and lesion samples from the 9 keloid patients. The average data output was 8,750,632,763 bp, and the average depth of each sample was 123×. The pathological tissue of Sample 2 had the highest sequencing depth (213.84×), followed by pathological Sample 8 (205.19×). The mean exome coverage of all the samples was 98.90%. Among them, the Sample 7 lesion tissue had the highest coverage (99.56%), followed by Sample 5 (99.53%) (see *Figure 1* and Table S1).

Identification of Somatic single nucleotide variants (SNPs), insertions/deletions (InDels), and copy number variations (CNVs)

We compared and analyzed the data of normal tissue samples from each patient with the data of paired keloid samples. By processing the sequencing data, we collected a total of 3,125 somatic SNVs and 299 InDels (see *Figure 1* and Table S2). Sample 8 had the most somatic SNVs [810], followed by Sample 1 [414]. The non-synonymous SNV types included stopgain and stoploss, and the non-synonym InDels mainly included frameshift deletions, frameshift insertions, and stop-gains (see *Figure 2*). CNVs were found in all the samples. The average CNV number of all the samples was 7,541, and the average CNV length was 7,314,569 bp. Sample 5 had the largest number of CNVs [15,431], followed by Sample 4 [12,873]. Sample 5 had the longest CNVs (14,862,648 bp), followed by Sample 4 (13,082,864 bp) (see *Figure 1* and Table S3).

We analyzed the variation of the somatic SNVs in patients from multiple perspectives, including mutation spectrums and mutation signatures. From these results, we were able to gain a clear understanding of the characteristics of keloid at the mutation level. The mutation spectrum analysis revealed a number of different types of keloid mutations and whether the samples have a preference for certain types of mutations. The characteristics of somatic point mutations in keloid can be studied by analyzing the spectrum and characteristics of somatic mutations. The analysis results showed that the main characteristics of keloid SNV were C > A and C > T (see *Figure 3*).

Significantly mutated genes (SMG) refer to mutation frequency of genes which is higher than the background significantly. Generally, the variation of SNVs and InDels in somatic cells is examined. MuSiC software (16) was used to identify higher frequencies of mutated genes in

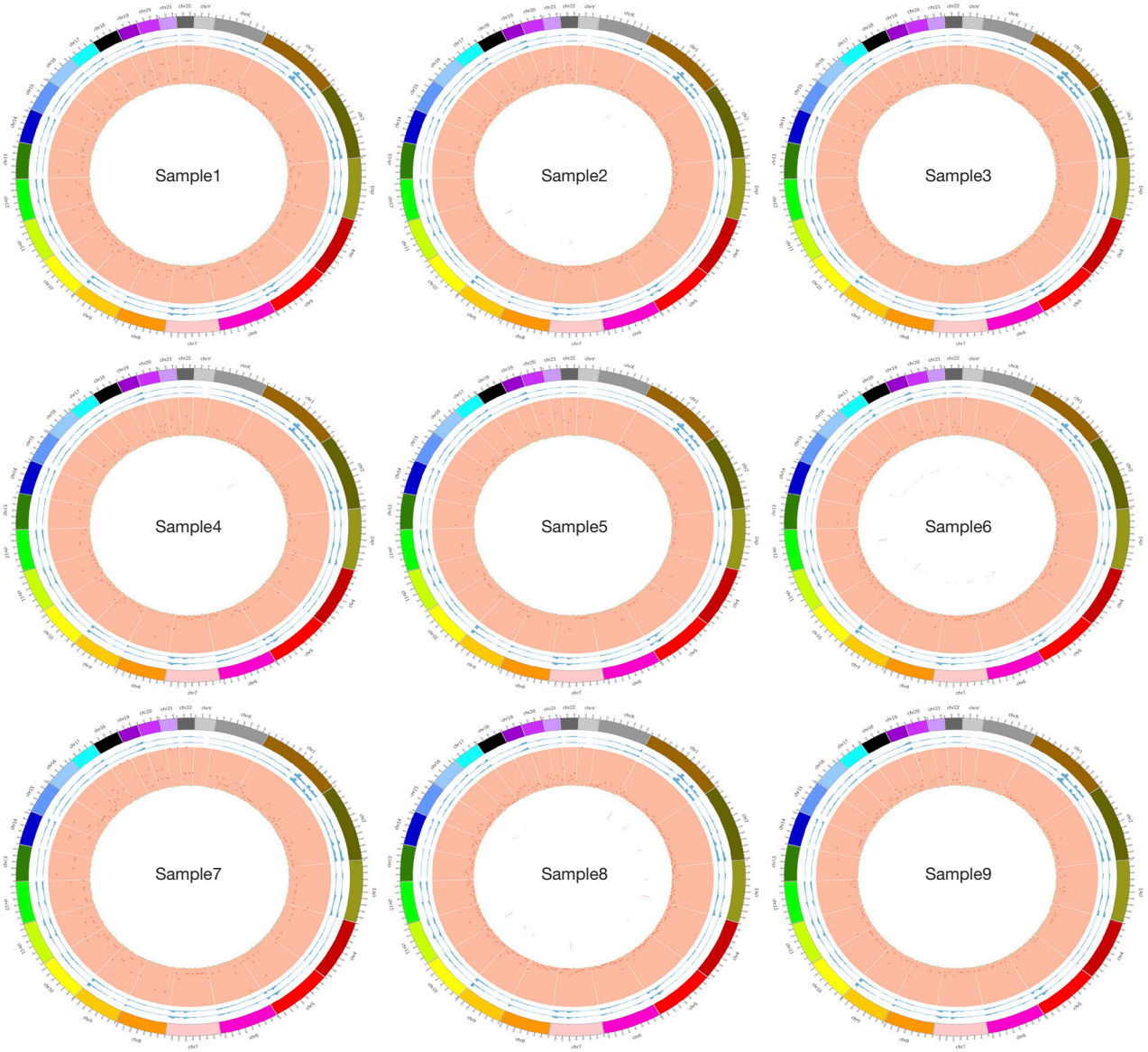

Figure 1 Global map of somatic variation in terms of cover depth, SNVs, InDels, and CNVs of all the samples. Circle 1: the outer frame of the chromosome. Circle 2: sequencing coverage map of the tumor samples. Circle 3: sequencing coverage map of the normal samples. Circle 4: the green dot represents the density of SNP InDel. Circle 5: CNV results; red indicates increased CNVs. Circle 6: CNV results; blue indicates missing CNVs. SNV, single nucleotide variant; InDel, insertions/deletion; CNV, copy number variation.

the keloid samples (compared to the normal skin samples), and statistical tests (e.g., the SMG test) were processed for each mutation type. The convolution-test (CT) method was used. We found that the highest frequencies of mutated genes included mucin 4 (MUC4) (55.6%),

tubulin tyrosine ligase like 12 (TTLL12) (33.3%), calcium voltage-gated channel subunit alpha1 C (CACNA1C) (33.3%), mucin 12 (MUC12) (33.3%). We identified the 30 genes with the highest mutation frequencies. The TMB of each sample was calculated separately, and the average TMB of each sample was 289 mutations/MB (see *Figure 4*).

KEGG and GO analyses

GO and KEGG pathway analyses were conducted for the

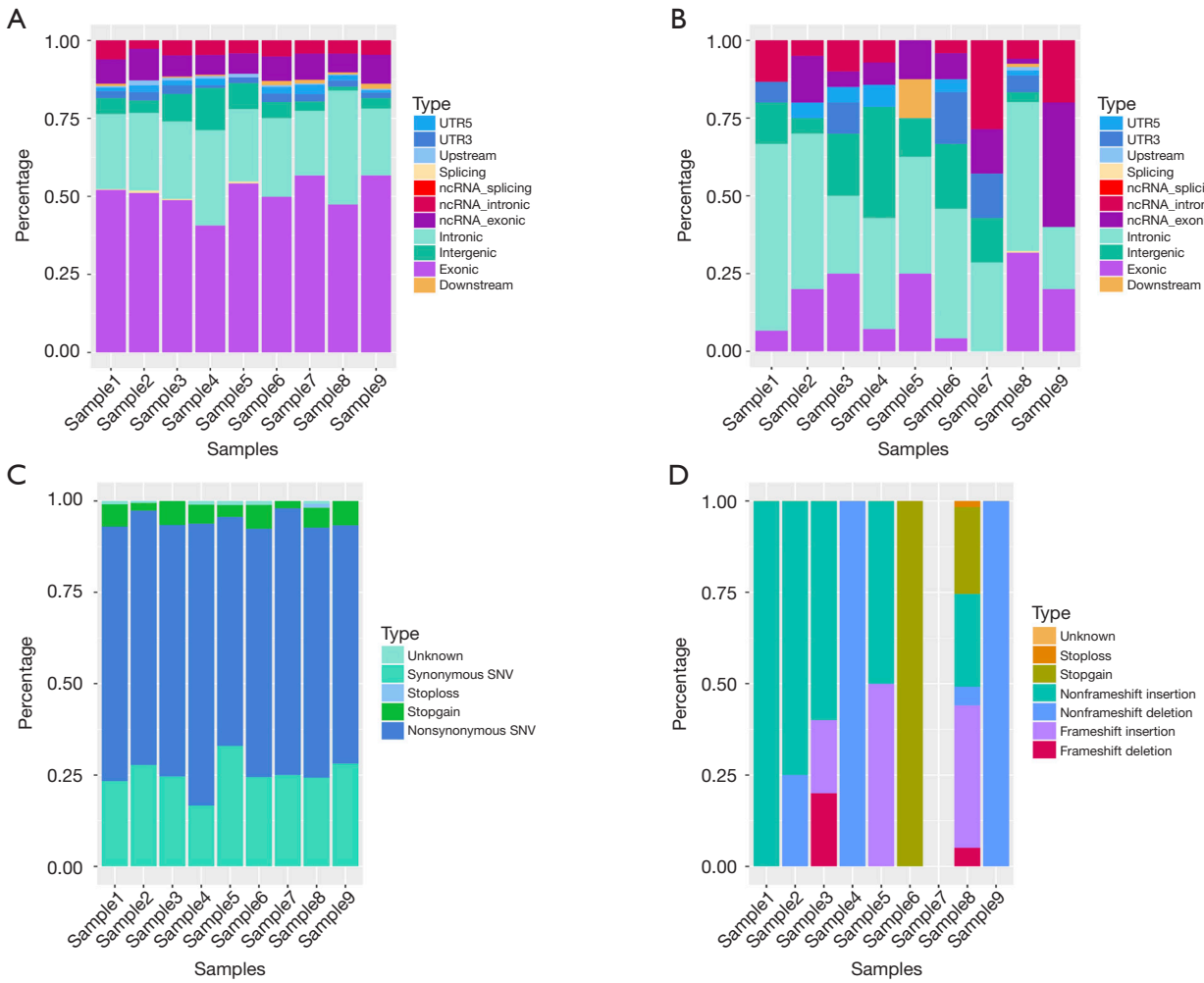

Figure 2 The distribution statistics of SNVs and InDels in the genome region, and the type statistics of SNV and InDel in the coding regions of all the samples. (A) Statistical distribution of SNVs in genomes of all the samples. (B) Statistical distribution of InDels in genomes of all the samples. (C) SNV type statistics for the coding regions of all the samples. (D) InDel type statistics for the coding region of all the samples. SNV, single nucleotide variant; InDel, insertions/deletion.

mutant genes. It was found that the mutant genes were mainly concentrated in GO binding cells, cell parts, and cellular processes (see *Figure 5A*). The KEGG pathway analysis showed that the mutant genes were mainly distributed in micro ribonucleic acids in cancer, the calcium signaling pathway, caffeine metabolism, extracellular matrix-receptor interactions, protein digestion and absorption (see *Figure 5B*).

Discussion

The pathogenesis of keloids is extremely complex, and keloids manifest in various forms (i.e., single or multiple). The causes of keloids include the patient's own factors (e.g., race, gene, age, and hormone level), site factors (e.g., local tension, active sites of sebaceous glands, and skin elasticity), and environmental factors (e.g., trauma and inflammation) (17). The treatment of keloid is difficult, and the treatment methods vary, but mainly include surgery, radiotherapy, steroids alone or combined with 5-FU local injection, laser, pressure therapy, and silicone patches. The effect of a combined treatment is better than that of any 1 treatment alone (18). As for the pathogenesis of keloids, no clear genetic factor has yet to be identified; thus, keloids may be caused by multiple gene polymorphisms (19).

There is a growing body of research focusing on the

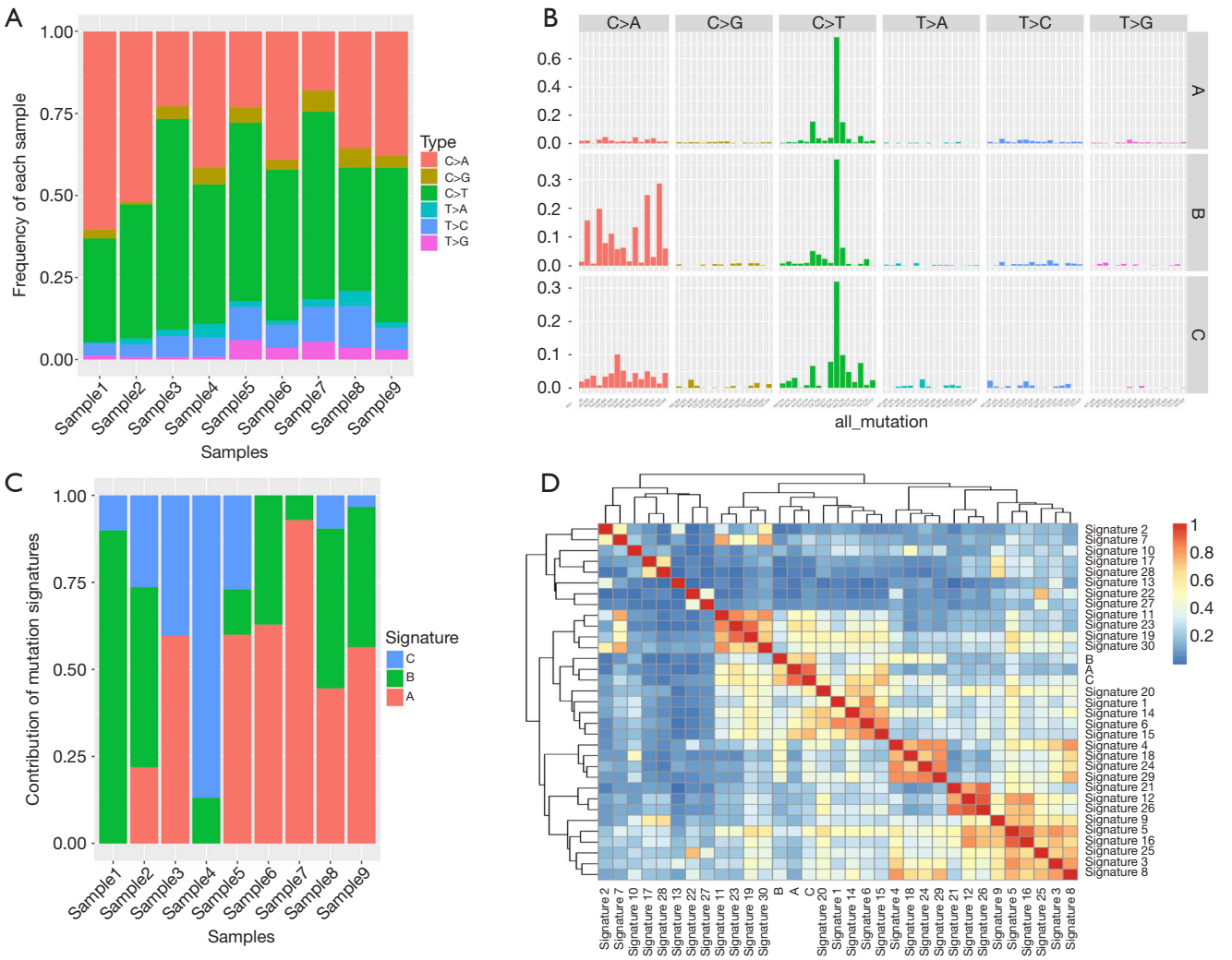

Figure 3 Mutant specificity of somatic SNVs in all the samples. (A) A heatmap of the mutation frequency of SNVs in all the samples. (B) Mutation profiles of SNVs in all the samples. (C) Mutation feature distribution map of all the samples. (D) Characteristic contrast heat map. SNV, single nucleotide variant.

epidermis and skin immune system (20,21). Cellular communication network factor 2 (CTGF), hepatocyte growth factor (HGF), and receptor C-MET have been detected in keloid keratinocytes. vascular endothelial growth factor (VEGF) and placental growth factor (PLGF), homeobox A7 (HOXA7), minichromosome maintenance 8 homologous recombination repair factor (MCM8), proteasome 20S subunit alpha 4 (PSMA4), and proteasome 20S subunit beta 2 (PSMB2) genes have been screened by functional tests (22-25). A previous study has also identified genes associated with epithelial differentiation, cell connectivity, and cell migration (26). In addition, a study has shown that epithelial mesenchymal transition also plays an important role in the development of keloids (27).

In this study, keloid skin tissues and paired normal skin tissues of 9 keloid patients were collected, and whole-exome sequencing and a related bioinformatics analysis were then performed. We attempted to observe the molecular mechanism of the occurrence and development of keloid from the genome level. We found high-frequency mutation genes, including *MUC4*, *TTLL12*, *CACNA1C*, and *MUC12*. *MUC4* was the highest frequently mutated gene. Mutations were found in the diseased tissues of 5 patients.

MUC4 is a highly glycosylated protein. It plays an

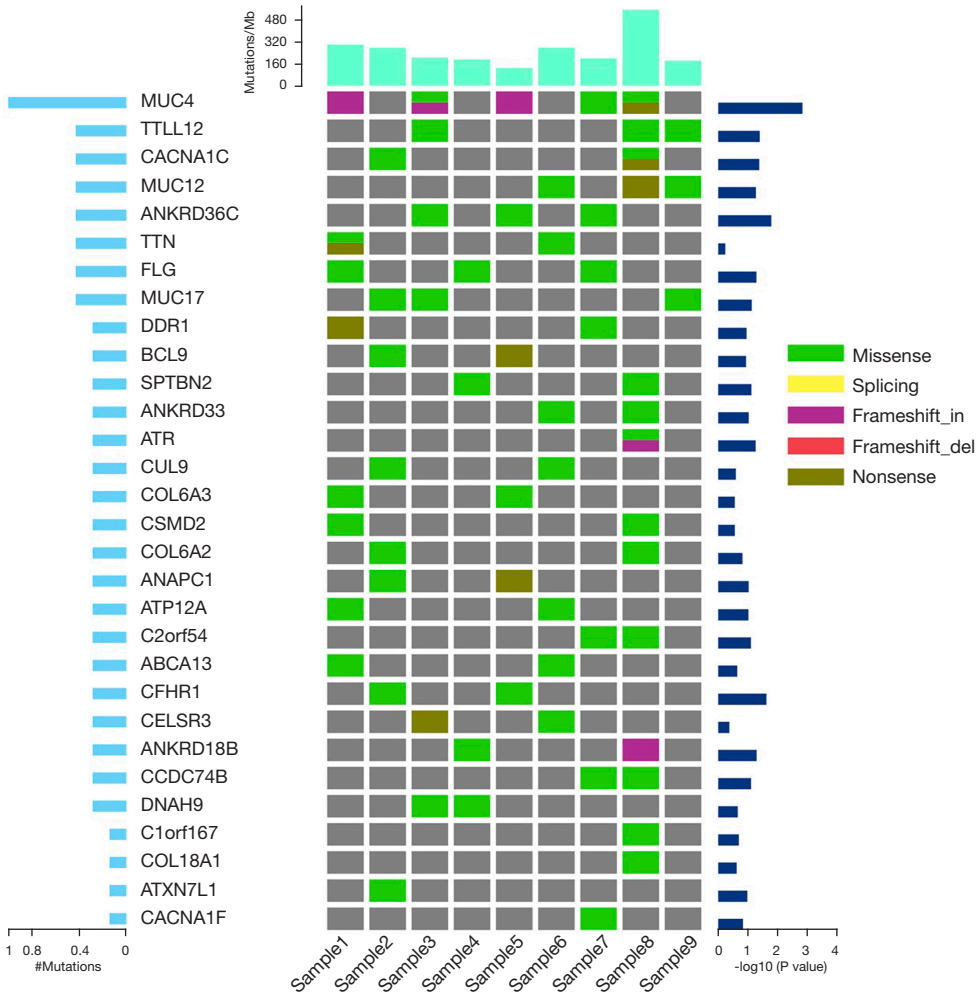

Figure 4 Survey of somatic mutations in all keloid patients. Left: proportion of the number of gene mutations. Right: significance of high-frequency mutations. Up: sample mutation frequency. The types of mutations are shown, including (I) non-synonymous mutations (green); (II) shear site mutations (yellow); (III) causes code shift insertions (purple); and (IV) causes code shift deletions (red).

important role in the protection of epithelial cells and is related to the regeneration and differentiation of epithelial cells. The gene encodes a complete membrane glycoprotein on the cell surface. There are at least 24 transcriptional variants of MUC4, some of which are found only in tumor tissues. MUC4 has been reported to be closely associated with the development of a variety of tumors (28). MUC4 expression is aberrantly upregulated in cutaneous squamous cell carcinomas (SCCs) (29,30), melanoma (31). High expression of MUC4 in SCC generally indicates a low tumor recurrence rate and a better prognosis (29). Since the expression of MUC4 in skin may be regulated by chronic inflammation (29), in keloid, there is a persistent inflammatory response, which may stimulate the over expression of MUC4. We speculated that the mutation of MUC4 also causes the abnormal regeneration and differentiation of epithelial cells, which reduces the protection of the skin and thus induces the production of keloids.

TTLL12 belongs to the tubulin tyrosine ligase family and plays an important role in tubulin modification, mitosis, and a variety of tumors. It has also been reported that TTLL12 regulates the innate immune antiviral signals (32,33), but this has not been reported in keloids. We believe that the variation of TTLL12 may lead to abnormal tubulin modifications that affect the normal division and structure of

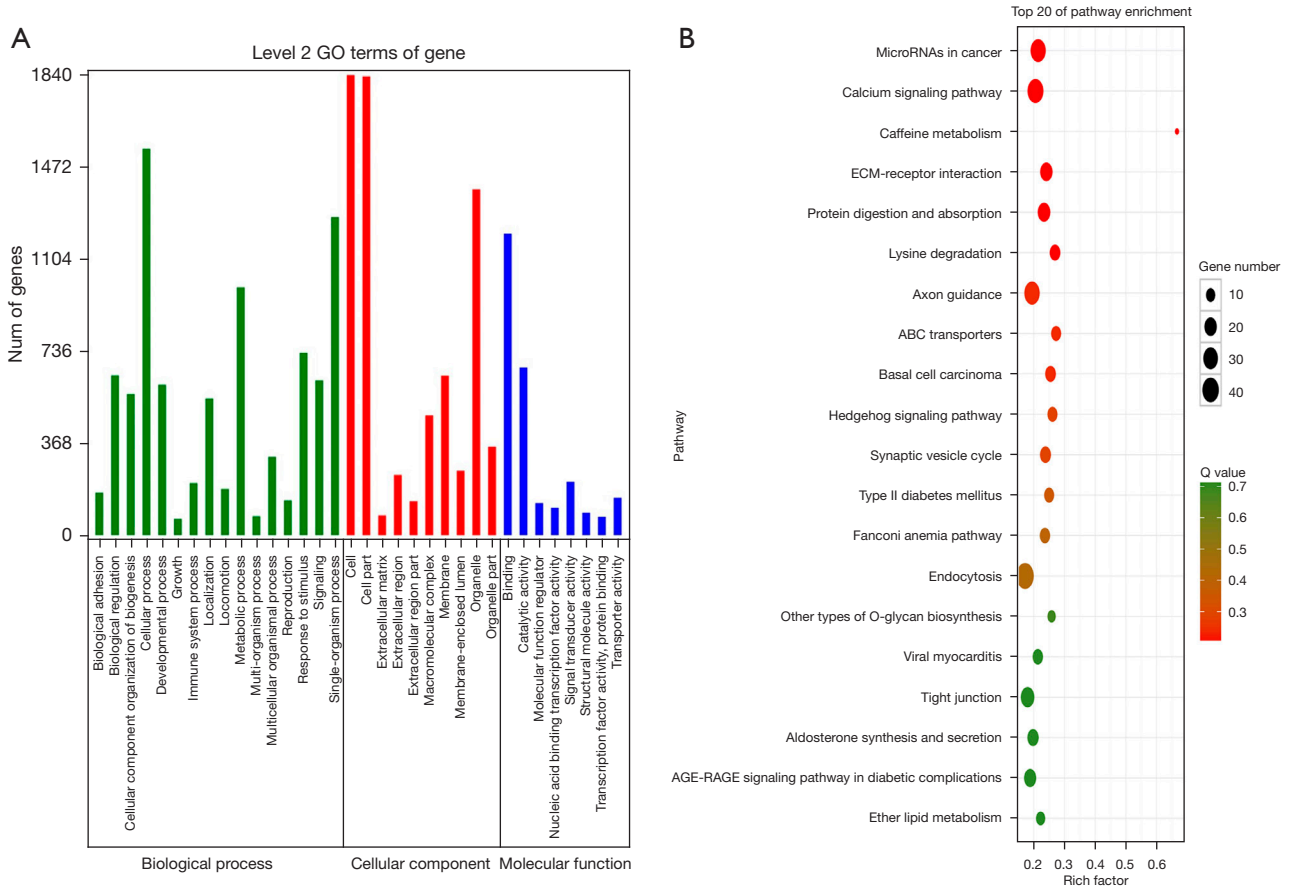

Figure 5 GO and KEGG analyses of all keloid patients. (A) GO analysis of all keloid patients. (B) KEGG analysis of mutant genes of all keloid patients. GO, Gene Ontology; KEGG, Kyoto Encyclopedia of Genes and Genomes.

epithelial cells, thus promoting the occurrence of keloids.

MUC12 encodes another complete membrane glycoprotein in the mucin family. MUC12 plays an important role in forming the protective mucosal barrier on the epithelial surface and intracellular signal transduction. MUC12 expression is downregulated in colorectal cancer tissues (34,35). There are mutations of MUC12 in human papillomavirus (HPV)-positive skin head and neck tumors (36). We hypothesize that the mutation of MUC12 weakens the protective mucosal barrier on the epithelial surface and cause abnormal intracellular signal transduction, thus making the skin more vulnerable to damage and causing keloids.

CACNA1C is T type α subunit of a calcium channel, function as tumor suppressors in cancer development, exhibited low expression in some tumor tissue (37), but the expression of CACNA1C in keloids has not been reported, the mutation of CACNA1C might cause unlimited cell proliferation in keloid and promote the growth of keloid.

In future work, we will verify the site of mutation, and conduct functional experiments on relevant genes.

Conclusions

Our study identified several genes involved in the development of keloids at the genomic level. These results may provide new strategies for the clinical management of keloid patients.

Acknowledgments

Funding: This work was supported by the Project of Nature Science Foundation of China (Nos. 82001978, 81702048 and 81703144).

Footnote

Reporting Checklist: The authors have completed the STREGA reporting checklist. Available at https://atm.amegroups.com/article/view/10.21037/atm-22-1303/rc

Data Sharing Statement: Available at https://atm.amegroups.com/article/view/10.21037/atm-22-1303/dss

Conflicts of Interest: All authors have completed the ICMJE uniform disclosure form (available at https://atm.amegroups.com/article/view/10.21037/atm-22-1303/coif). The authors have no conflicts of interest to declare.

Ethical Statement: The authors are accountable for all aspects of this work, including ensuring that any questions related to the accuracy or integrity of any part of the work have been appropriately investigated and resolved. This study was conducted in accordance with the Declaration of Helsinki (as revised in 2013), and was approved by the Ethics Committee of The First Affiliated Hospital of Soochow University (application No. 2022014). Informed written consent was provided by all patients before their inclusion in this study.

References

1. Qu M, Song N, Chai G, et al. Pathological niche environment transforms dermal stem cells to keloid stem cells: a hypothesis of keloid formation and development. Med Hypotheses 2013;81:807-12.
2. Rockwell WB, Cohen IK, Ehrlich HP. Keloids and hypertrophic scars: a comprehensive review. Plast Reconstr Surg 1989;84:827-37.
3. Kiprono SK, Chaula BM, Masenga JE, et al. Epidemiology of keloids in normally pigmented Africans and African people with albinism: population-based cross-sectional survey. Br J Dermatol 2015;173:852-4.
4. Seifert O, Mrowietz U. Keloid scarring: bench and bedside. Arch Dermatol Res 2009;301:259-72.
5. Yi H, Liao ZW, Chen JJ, et al. Genome variation in colorectal cancer patient with liver metastasis measured by whole-exome sequencing. J Gastrointest Oncol 2021;12:507-15.
6. Smolle E, Taucher V, Lindenmann J, et al. Liquid biopsy in non-small cell lung cancer-current status and future outlook-a narrative review. Transl Lung Cancer Res 2021;10:2237-51.
7. Chen D, Wang R, Yu C, et al. FOX-A1 contributes to acquisition of chemoresistance in human lung adenocarcinoma via transactivation of SOX5. EBioMedicine 2019;44:150-61.
8. Mann GJ, Pupo GM, Campain AE, et al. BRAF mutation, NRAS mutation, and the absence of an immune-related expressed gene profile predict poor outcome in patients with stage III melanoma. J Invest Dermatol 2013;133:509-17.
9. Berger MF, Hodis E, Heffernan TP, et al. Melanoma genome sequencing reveals frequent PREX2 mutations. Nature 2012;485:502-6.
10. Li Y, Li M, Qu C, et al. The Polygenic Map of Keloid Fibroblasts Reveals Fibrosis-Associated Gene Alterations in Inflammation and Immune Responses. Front Immunol 2022;12:810290.
11. Li H, Durbin R. Fast and accurate long-read alignment with Burrows-Wheeler transform. Bioinformatics 2010;26:589-95.
12. Cibulskis K, Lawrence MS, Carter SL, et al. Sensitive detection of somatic point mutations in impure and heterogeneous cancer samples. Nat Biotechnol 2013;31:213-9.
13. Kanehisa M, Goto S. KEGG: kyoto encyclopedia of genes and genomes. Nucleic Acids Res 2000;28:27-30.
14. Ashburner M, Ball CA, Blake JA, et al. Gene ontology: tool for the unification of biology. The Gene Ontology Consortium. Nat Genet 2000;25:25-9.
15. Weaver B, Wuensch KL. SPSS and SAS programs for comparing Pearson correlations and OLS regression coefficients. Behav Res Methods 2013;45:880-95.
16. Dees ND, Zhang Q, Kandoth C, et al. MuSiC: identifying mutational significance in cancer genomes. Genome Res 2012;22:1589-98.
17. Limandjaja GC, Niessen FB, Scheper RJ, et al. The Keloid Disorder: Heterogeneity, Histopathology, Mechanisms and Models. Front Cell Dev Biol 2020;8:360.
18. Ogawa R. Keloid and Hypertrophic Scars Are the Result

of Chronic Inflammation in the Reticular Dermis. Int J Mol Sci 2017;18:606.
19. Glass DA 2nd. Current Understanding of the Genetic Causes of Keloid Formation. J Investig Dermatol Symp Proc 2017;18:S50-3.
20. Limandjaja GC, van den Broek LJ, Waaijman T, et al. Increased epidermal thickness and abnormal epidermal differentiation in keloid scars. Br J Dermatol 2017;176:116-26.
21. Jin Q, Gui L, Niu F, et al. Macrophages in keloid are potent at promoting the differentiation and function of regulatory T cells. Exp Cell Res 2018;362:472-6.
22. Khoo YT, Ong CT, Mukhopadhyay A, et al. Upregulation of secretory connective tissue growth factor (CTGF) in keratinocyte-fibroblast coculture contributes to keloid pathogenesis. J Cell Physiol 2006;208:336-43.
23. Mukhopadhyay A, Fan S, Dang VD, et al. The role of hepatocyte growth factor/c-Met system in keloid pathogenesis. J Trauma 2010;69:1457-66.
24. Ong CT, Khoo YT, Tan EK, et al. Epithelial-mesenchymal interactions in keloid pathogenesis modulate vascular endothelial growth factor expression and secretion. J Pathol 2007;211:95-108.
25. Li M, Wu L. Functional analysis of keratinocyte and fibroblast gene expression in skin and keloid scar tissue based on deviation analysis of dynamic capabilities. Exp Ther Med 2016;12:3633-41.
26. Hahn JM, Glaser K, McFarland KL, et al. Keloid-derived keratinocytes exhibit an abnormal gene expression profile consistent with a distinct causal role in keloid pathology. Wound Repair Regen 2013;21:530-44.
27. Stone RC, Pastar I, Ojeh N, et al. Epithelial-mesenchymal transition in tissue repair and fibrosis. Cell Tissue Res 2016;365:495-506.
28. Wang S, You L, Dai M, et al. Quantitative assessment of the diagnostic role of mucin family members in pancreatic cancer: a meta-analysis. Ann Transl Med 2021;9:192.
29. Chakraborty S, Swanson BJ, Bonthu N, et al. Aberrant upregulation of MUC4 mucin expression in cutaneous condyloma acuminatum and squamous cell carcinoma suggests a potential role in the diagnosis and therapy of skin diseases. J Clin Pathol 2010;63:579-84.
30. Kathpalia VP, Mussak EN, Chow SS, et al. Genome-wide transcriptional profiling in human squamous cell carcinoma of the skin identifies unique tumor-associated signatures. J Dermatol 2006;33:309-18.
31. Yu J, Xu L, Yan J, et al. MUC4 isoforms expression profiling and prognosis value in Chinese melanoma patients. Clin Exp Med 2020;20:299-311.
32. Ju LG, Zhu Y, Lei PJ, et al. TTLL12 Inhibits the Activation of Cellular Antiviral Signaling through Interaction with VISA/MAVS. J Immunol 2017;198:1274-84.
33. Wasylyk C, Zambrano A, Zhao C, et al. Tubulin tyrosine ligase like 12 links to prostate cancer through tubulin posttranslational modification and chromosome ploidy. Int J Cancer 2010;127:2542-53.
34. Jiang Z, Wang H, Li L, et al. Analysis of TGCA data reveals genetic and epigenetic changes and biological function of MUC family genes in colorectal cancer. Future Oncol 2019;15:4031-43.
35. Matsuyama T, Ishikawa T, Mogushi K, et al. MUC12 mRNA expression is an independent marker of prognosis in stage II and stage III colorectal cancer. Int J Cancer 2010;127:2292-9.
36. Nichols AC, Chan-Seng-Yue M, Yoo J, et al. A Pilot Study Comparing HPV-Positive and HPV-Negative Head and Neck Squamous Cell Carcinomas by Whole Exome Sequencing. ISRN Oncol 2012;2012:809370.
37. Phan NN, Wang CY, Chen CF, et al. Voltage-gated calcium channels: Novel targets for cancer therapy. Oncol Lett 2017;14:2059-74.

(English Language Editor: L. Huleatt)

Cite this article as: Zhu YQ, Zhou NH, Xu YW, Liu K, Li W, Shi LY, Hu YX, Xie YF, Lan J, Yu ZY. Genome-wide analysis of Chinese keloid patients identifies novel causative genes. Ann Transl Med 2022;10(16):883. doi: 10.21037/atm-22-1303

Supplementary

Table S1 Sequencing data summary of all samples

Sample ID	Mapped target base	Average target depth	Total near target base	Mapped near target base	Average near target depth	Near target coverage ratio (%)	Target coverage ratio (%)	Target coverage 5× (%)	Target coverage 10× (%)	Target coverage 20× (%)	Target coverage 50× (%)	Target coverage 100× (%)
Sample1-ks	9.7E+09	160.45	76180188	1.78E+09	23.4	76.2	99.25	98.8	98.3	97.11	91.28	72.02
Sample1-ns	9.6E+09	158.82	76180188	1.71E+09	22.43	74.27	99.05	98.3	97.49	95.77	88.99	70.53
Sample2-ks	1.29E+10	213.84	76180188	2.24E+09	29.4	66	96.87	91.03	86.31	81.21	73.1	62.7
Sample2-ns	9.36E+09	154.75	76180188	1.9E+09	24.94	81.53	99.25	98.77	98.24	97.05	91.14	70.86
Sample4-ks	5.19E+09	85.87	76180188	9.39E+08	12.33	67.26	98.95	97.93	96.56	93.01	74.58	32.81
Sample4-ns	9.01E+09	149.07	76180188	1.64E+09	21.47	75.23	99.38	98.86	98.29	96.93	90.36	68.93
Sample8-ns	7.4E+09	122.35	76180188	1.36E+09	17.83	73.13	99.17	98.52	97.73	95.79	86.31	57.48
Sample8-ks	1.24E+10	205.19	76180188	2.02E+09	26.47	67.04	99.14	97.02	92.86	83.69	68.56	56.81
Sample7-ks	8.44E+09	139.57	76180188	1.54E+09	20.18	74.93	99.56	99.08	98.48	96.98	89.19	64.61
Sample7-ns	6.86E+09	113.5	76180188	1.34E+09	17.6	75.74	99.4	98.74	97.91	95.79	84.67	52.03
Sample5-ks	8.91E+09	147.3	76180188	1.68E+09	22.05	77.49	99.53	99.07	98.51	97.17	90.15	67.28
Sample5-ns	1.09E+10	180.35	76180188	1.99E+09	26.14	73.89	98.06	95.45	93.39	90.27	81.84	66.64
Sample6-ks	7.27E+09	120.27	76180188	1.31E+09	17.14	71.28	99.38	98.79	97.97	95.72	82.83	51.51
Sample6-ns	8.52E+09	140.91	76180188	1.34E+09	17.63	58.48	99.21	96.24	89.86	73.54	45.73	33.33
Sample9-ks	7.13E+09	117.9	76180188	1.33E+09	17.42	74	99.25	98.69	97.99	96.01	83.97	50.93
Sample9-ns	6.39E+09	105.73	76180188	1.14E+09	14.91	70.41	99.23	98.62	97.8	95.33	80.01	43.38

https://dx.doi.org/10.21037/atm-22-1303

Table S2 The number summary of all samples CNVs and InDels

Sample name	SNV number	InDel number
Sample 1	414	15
Sample 2	374	20
Sample 3	251	20
Sample 4	238	14
Sample 5	169	8
Sample 6	370	24
Sample 7	261	7
Sample 8	810	186
Sample 9	238	5

CNVs, copy number variations; InDel, insertions/deletion.

Table S3 Summary of all samples CNVs

Sample	Gain number	Gain length	Loss number	Loss length	Total number	Total length
Sample 5	6	3817	15425	14858831	15431	14862648
Sample 4	0	0	12873	13082864	12873	13082864
Sample 3	2	1378	9952	10131422	9954	10132800
Sample 2	10861	10100743	17	13369	10878	10114112
Sample 8	5583	5053630	24	22205	5607	5075835
Sample 7	4685	4899591	7	4873	4692	4904464
Sample 6	22	20942	4649	4076135	4671	4097077
Sample 1	2100	2113612	114	84958	2214	2198570
Sample 9	1536	1350963	17	11795	1553	1362758

CNVs, copy number variations.

https://dx.doi.org/10.21037/atm-22-1303